

**Analysis of 50-year wind
data of the southern
Baltic Sea for modelling
coastal morphological
evolution – a case study
from the Darss-Zingst
Peninsula**

OCEANOLOGIA, 53 (1-TI), 2011.
pp. 489–518.

© 2011, by Institute of
Oceanology PAS.

KEYWORDS

Representative wind series
Statistical analysis
Morphodynamic model
Southern Baltic Sea

WENYAN ZHANG^{1,*}

JAN HARFF²

RALF SCHNEIDER¹

¹ Institute of Physics,
Ernst-Moritz-Arndt University of Greifswald,
Felix-Hausdorff-Str. 6, Greifswald 17489, Germany;

e-mail: wzhang@ipp.mpg.de

*corresponding author

² Institute of Marine and Coastal Sciences,
Szczecin University,
Adama Mickiewicza 18, Szczecin 70–383, Poland

Received 6 October 2010, revised 1 March 2011, accepted 2 March 2011.

Abstract

High-resolution wind series in the southern Baltic Sea for the period of 1958–2007 are analysed to generate representative climate input conditions for a multi-scale morphodynamic model to simulate decadal-to-centennial coastline change. Four seasonal wind classes, each characterized by a predominant distribution of wind direction and speed, are derived from statistical analysis. Further calibration of this statistical description is done by sensitivity studies of the model to generate similar coastline changes of the Darss-Zingst peninsula as the measured data for the last century. The coastline change of this area is then projected for the next 300 years based on four different climate scenarios, through which impacts of accelerated sea level rise and storm frequency on the long-term coastline change are quantified.

1. Introduction

Following the onset of the Littorina transgression (approximately 8000 cal BP), the sea level in the southern Baltic Sea has reached a relatively stable

The complete text of the paper is available at <http://www.iopan.gda.pl/oceanologia/>

level with minor fluctuations in the range of only a few metres in the last 6000 years (Kliewe 1995, Schumacher & Bayerl 1999). The rate of sea level change (in this study, the term ‘sea level change’ refers only to eustatic change) has generally been between -1 mm year^{-1} and 1 mm year^{-1} in the southern Baltic Sea in the last 4000 years according to the results of Lampe (2005), which is of the same order of magnitude as the neotectonic movements in this area (Harff et al. 2007). Along with the stable sea level and neotectonic conditions, other processes such as climate change, hydrodynamics and sediment transport have become increasingly important for coastline evolution (Schwarzer & Diesing 2003).

In contrast to other waters, the Baltic Sea is distinguished by its great variety of coastal types. In general, till material predominates along the southern and south-eastern coasts, while hard-bottom and rocky shores are typical on northern coasts (Schiewer 2008). The Baltic Sea can be described as a tideless semi-enclosed marginal sea. The hydrodynamics of the Baltic is characterized mainly by complicated meso-to-large scale wind-driven currents and local-scale wind-induced waves. Tides coming from the North Sea attenuate quickly after entering the Baltic Sea through a series of narrow channels. The tidal range in the southern Baltic area is no more than 15 cm, while large-scale meteorological situations can excite a storm surge with

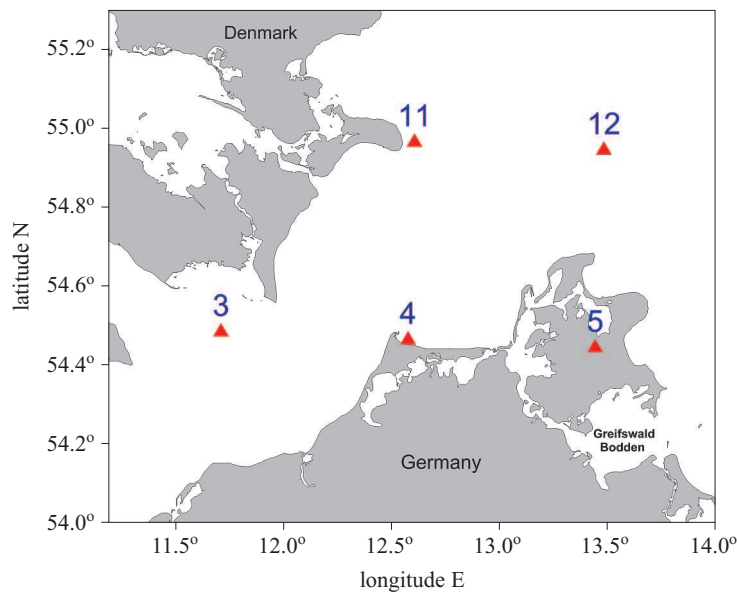


Figure 1. General features and location of the Darss-Zingst peninsula. Hindcasted wind series at five points (triangles) are analysed to generate the representative wind inputs for the long-term model

water level changes of the order of 1.5 m within one day. The Darss-Zingst peninsula (Figure 1) on the southern Baltic was formed after the postglacial transgression (Schumacher 2002, Lampe 2002) and is composed of two main parts. The exterior part is a triangularly shaped barrier island with two 'wings' extending south-westwards (Fischland-Darss) and eastwards (Darss-Zingst), and a headland (Darsser Ort) linking the two wings in the north. The formation of the barrier island is the result of a combination of climate change, hydrodynamics and sediment transport, which still remains active today. The interior part consists of a chain of lagoons (the 'Darss-Zingst Bodden'), which are subject to progressive phytogenic silting-up. The westerly exposed coast of Darss and the northerly exposed coast of Zingst are characterized by strong abrasion of the cliff coast and the flat beach coast, as well as a rapid accumulation at the top of the headland (Darsser Ort) as a result of the abundant sediment supply brought by the wind-induced longshore currents. The eastern extension of the peninsula is the 'Bock' sand flat, which is separated from the southernmost tip of Hiddensee Island by a dredged channel. Bock Island is like a container, where sediment transported southwards along Hiddensee and eastwards along the Zingst coast accumulates. The particular evolution of the Darss-Zingst peninsula may serve as a good example to study coastal evolution under long-term climate change, and has instigated several descriptive and conceptual studies in the last 100 years (Otto 1913, Kolp 1978, Lampe 2002, Schumacher 2002).

In contrast to traditional geological and sedimentological studies based on field observation and analysis, morphodynamic modelling of coastal evolution based on process concepts is in its infancy, owing to its dependence on computer power, which has only recently become available. Process-based models can be divided into three categories according to their object of study on different time scales: (1) real-time simulation on time scales from tidal to seasonal periods, (2) medium long-term simulation on time scales from annual, decadal to centennial and millennial periods, and (3) extreme long-term or geological time scale (longer than 10 000 years scale) simulation. Models for the first and third category are well developed today and a wide range of such models is available. However, the development of models for the second category (hereafter referred to as 'long-term model') has yet to reach maturity (Fagherazzi & Overeem 2007). A common way of simulating decadal-to-centennial coastal morphological evolution is to extrapolate the real-time calculation (the first type of model) to longer time periods. However, poor results are usually obtained when these models are applied directly on such a time scale. This is due mainly to three reasons: (1) the time step of calculation in high-resolution process-based models (the first type of model) is determined by the shortest time-scale

process, i.e. usually of the order of seconds or minutes, and truncation errors generated after each calculation time step can accumulate during continuous run cycles in a long-term model, giving rise to substantial bias between the final simulation results and reality; (2) detailed time series of data (e.g. flows, waves and sediment) covering such a long time span serving as model boundary input are absent; and (3) the variation of bathymetry occurring in a stochastically short time period, e.g. in a wind storm period, may exceed the change in a longer time span (1 year). One way of bridging the gap between the simulation of short-term hydrodynamics, sediment transport and morphological changes taking place over much longer timescales is to integrate the concepts of ‘reduction’ (de Vriend et al. 1993a,b, Latteaux 1995) and techniques of morphological update acceleration (Roelvink 2006, Jones et al. 2007) into high-resolution process-based models. Three approaches can be derived from the ‘reduction’ strategy: (1) model reduction, in which only the main driving terms on the scale of interest are considered, while small scale processes that can be smoothed over a longer time period are avoided or integrated into an average term; (2) input reduction, in which the input data should be refined into some representative data groups capable of producing similar results as the whole variety of real time series on the scale of interest; and (3) behaviour-based models, in which small scale processes are replaced by observational knowledge. By ‘extracting’ the most important processes responsible for the long-term coastal morphological evolution based on the concepts of ‘reduction’ and combining the technique of morphological update acceleration, high-resolution process-based models are applied to long-term simulation. Decadal tidal inlet change (Cayocca 2001, Dissanayake & Roelvink 2007), decadal micro-tidal spit-barrier development (Jiménez & Arcilla 2004), millennial tidal basin evolution (Dastgheib et al. 2008) and millennial delta evolution (Wu et al. 2006) were all simulated by such models, in which promising results were obtained.

Recently, a modeling methodology was developed by the authors for simulating the decadal-to-centennial morphological evolution of wave-dominated barrier islands in the southern Baltic Sea (Zhang et al. 2010). The methodology consists of two main components: (1) a preliminary analysis of the key processes driving the morphological evolution of the study area based on statistical analysis of meteorological data and sensitivity studies, and (2) a multi-scale process-based morphodynamic model, in which the ‘reduction’ concepts and techniques for morphological update acceleration are implemented. The model is validated by comparison between measured data and simulated coastline change of the Darss-Zingst peninsula for the last 300 years. A detailed description of the model

construction and its modeling strategy for a long-term scale is introduced in Zhang et al. (2010). In this paper we introduce mainly the concepts of representative climate input conditions for the morphodynamic model and the methodology for generating representative climate input conditions. The coastline changes of this area in the next 300 years, based on four different climate scenarios derived from different studies, are then projected by the model, through which the impacts of accelerated sea level rise and storm frequency on long-term coastline change are quantified.

2. Material and methods

2.1. Brief description of the model

Simulation of the decadal-to-centennial morphological evolution of the Darss-Zingst peninsula is based on a multi-scale morphodynamic model consisting of 8 modules to calculate different physical processes that drive the evolution of the specific coastal environment. The two-dimensional vertically integrated circulation module, the wave module, the bottom boundary layer module, the sediment transport module, the cliff erosion module and the nearshore storm module are real-time calculation modules that aim to solve short-term processes. A bathymetry update module and a long-term control function set, in which the ‘reduction’ concepts and technique for morphological update acceleration are implemented, are integrated to up-scale the effects of short-term processes to a decadal-to-centennial scale.

2.2. Wind analysis

Boundary input conditions for a long-term (decadal-to-centennial) morphodynamic model such as time series of tides, winds, waves and mass flux cannot be specified at a centennial time span owing to the lack of measurements. On the other hand, even if detailed, measured time series of boundary conditions were provided, it would be an extremely time-consuming job for a high-resolution process-based model to calculate the centennial-scale coastal evolution with the measured time series. This is because the time step of calculation in high-resolution process-based models is determined by the shortest time scale process, which usually has to be solved on a time scale of seconds or minutes. Representative input conditions, which are generated by the statistical analysis of the measured time series, provide an effective way of solving the input problem for the long-term model. The generation of representative input conditions is based on the concept of ‘input reduction’ for long-term modelling (de Vriend et al. 1993a,b). The criterion for judging the validity of the representative input

conditions is whether the simulation results based on the representative input conditions are the same as the reference data. As the effects of tides can be neglected in the southern Baltic Sea, only the time series of winds are needed for generating the representative input conditions. In this study we use the hindcast high-resolution wind series (covering the southern Baltic area with a spatial resolution of $50 \text{ km} \times 50 \text{ km}$) from 1958 to 2007 (provided by Weisse, GKSS-Research Centre, Geesthacht) to generate the representative wind conditions. The hourly wind series result from a hindcast in which the regional atmosphere model is driven with the NCEP/NCAR global re-analysis in combination with spectral nudging. A detailed description of the atmosphere model and its validation are given by Weisse & Guenther (2007) and Weisse et al. (2009).

The hindcast wind series at five points covering the Darss-Zingst peninsula are analysed (Figure 1). The differences of wind time series among these points can be measured by the RMSE (Root Mean Square Error):

$$\text{RMSE}_{X,Y} = \frac{\sqrt{\sum_{i=1}^N (y_i - \chi_i)^2}}{\sqrt{N}}, \quad (1)$$

where $X = \{\chi_i\}$, $Y = \{y_i\}$ are two separate data sets, each of N elements.

By using the hourly wind series at Point 3 as the reference data, RMSE between the wind series at this point and other points are calculated and listed in Table 1. Here u represents the east-west component of the wind (positive towards the east) and v represents the north-south component of the wind (positive towards the north). Results indicate that the wind time series at these points are quite similar.

Table 1. RMSE of hourly wind time series between Point 3 and other points on the Darss-Zingst peninsula for the period 1958–2007

Point	RMSE of u with Point3 [m s^{-1}]	RMSF of v with Point3 [m s^{-1}]
4	0.39	0.27
5	0.51	0.41
11	0.79	0.55
12	1.03	0.67

2.2.1. Generation of representative wind series

As the hourly wind series at the five adjacent points are quite similar, we introduce here mainly the results of the statistical analysis at Point 3 as this point is closest to the western boundary of the local model, and statistical

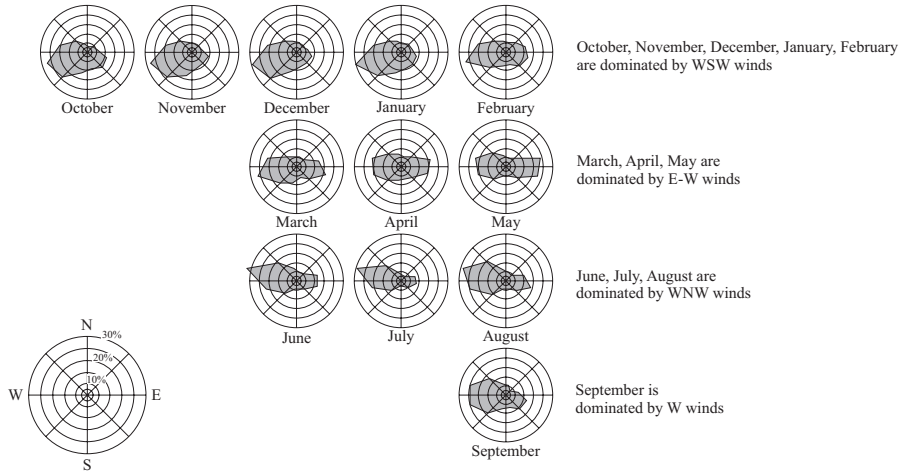


Figure 2. Four wind classes, each with a predominant wind direction, are classified from the wind roses of 12 months based on the data from 1958 to 2007

results indicate that the wind time series at Point 3 is closest to the mean value of the series at the five points (with a value of 0.34 m s^{-1} for the RMSE of component u and 0.22 m s^{-1} for the RMSE of component v). Statistical results indicate that the southern Baltic Sea is dominated by westerly winds and the 50 year-averaged wind speed is 7.5 m s^{-1} in the Darss-Zingst area. The ratio of westerly winds (hours) to easterly winds (hours) is about 18:11. The distribution of wind directions of each month in this period shows that the winds in the Darss-Zingst area can be classified into four seasonal classes (Figure 2). Each class has a predominant distribution of wind direction. By combining the monthly average wind speed profiles, Class 1 (October, November, December, January and February) can be identified as a winter class with relatively strong wind conditions; the prevailing wind direction is WSW. Class 3 (June, July and August) can be identified as a summer class with mild wind conditions dominated by the WNW winds. Class 2 (March, April and May) and Class 4 (September) are transitional classes with moderate wind conditions. Class 2 is dominated by the East-West balanced winds and Class 4 is dominated by westerly winds. The Weibull distribution is utilized to analyse the wind strength. The Weibull distribution function is a two-parameter function, for wind speed

$$f(\chi \geq 0; k, \lambda) = \frac{k}{\lambda} \left(\frac{\chi}{\lambda}\right)^{k-1} \exp \left[- \left(\frac{\chi}{\lambda}\right)^k \right], \quad (2)$$

where f is the probability density function (PDF) of the wind speed, χ represents the wind speed, $k > 0$ is the shape parameter, and $\lambda > 0$ is the

scale parameter. The cumulative distribution function is given by

$$F(\chi) = 1 - \exp \left[- \left(\frac{\chi}{\lambda} \right)^k \right]. \quad (3)$$

With a double logarithmic transformation, eq. (3) can be written as

$$\ln\{-\ln[1 - F(\chi)]\} = k \ln \chi - k \ln \lambda. \quad (4)$$

Knowing $F(\chi)$ and χ from the wind speed data, the value of k and λ can be determined by least squares fitting using eq. (4).

Table 2. Monthly long-term shape parameters k , scale parameters λ and Pearson's Chi-square χ^2 of the Weibull distribution at Point 3 for the period 1958–2007

Month	Shape (k) with Point3 [m s ⁻¹]	Scale (λ) with Point3 [m s ⁻¹]	χ^2
Jan.	2.44	9.40	0.015
Feb.	2.41	8.97	0.015
March	2.29	8.52	0.018
April	2.24	7.16	0.021
May	2.22	6.70	0.019
June	2.17	6.66	0.022
July	2.12	6.84	0.021
Aug.	2.20	6.87	0.019
Sept.	2.27	7.61	0.023
Oct.	2.40	8.89	0.017
Nov.	2.51	9.29	0.016
Dec.	2.52	9.37	0.011

The Weibull parameters for each month (Table 2) are obtained by applying eq. (4) to the 50-year wind series. Pearson's Chi-square test is used to evaluate the performance of the Weibull fitting, which is given by

$$\chi^2 = \sum_{i=1}^N (O_i - E_i)^2 / E_i, \quad (5)$$

where O_i is the measured frequency for bin i (the wind speed data is divided into 60 bins at intervals of 0.5 m s⁻¹), and E_i is the expected frequency for bin i , which is calculated by

$$E_i = k(F(i/2) - F(i/2 - 0.5)), \quad (6)$$

where k is the size of the wind speed series, and F is the cumulative distribution function given by eq. (3).

Results of Pearson's Chi-square test show satisfactory fitting of the Weibull distribution to the wind data (Table 2). Weibull parameters for

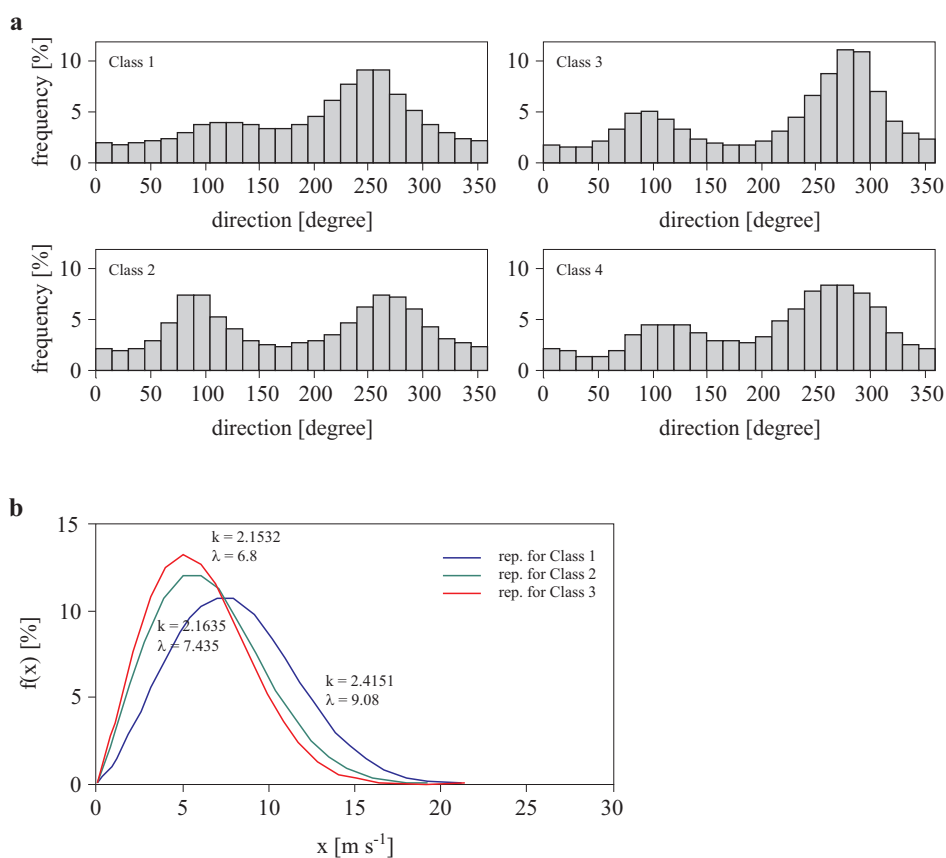


Figure 3. (a) Distribution of wind directions for each class: 90° indicates an easterly wind and 270° a westerly wind; (b) the Weibull distribution of wind speeds for each class

the months in Class 1 indicate their similar distributions of wind strength. The months in Class 3 also have similar Weibull parameters. The Weibull parameters of the three months in Class 2 indicate a decreasing trend of wind strength. The average term of the wind strength of this class is reflected in the April distribution. Based on the similarities of the monthly Weibull parameters within the same class, the Weibull distribution for each class is obtained by applying eq. (4) to the wind series of the months within the same class. The results are shown in Figure 3b (parameters of Class 4 are not shown as they are already listed in Table 2). The concept of ‘representative’ monthly wind series is introduced in this study. A representative monthly wind series is composed of 720 (hours in a month) synthetic wind elements. This is able to reflect statistically the features (spectrum) of a wind class, and thus represents the months of one class. The use of representative

monthly wind series is related to the strategy of morphological update (Zhang et al. 2010). The model calculates one representative wind series instead of all the months it represents; thus, it is able to save CPU time. Based on the Weibull parameters for each class, the representative monthly wind series are derived through the following procedures:

- (1) Four wind classes are used to generate their corresponding representative monthly wind series. Wind speeds of each representative series are given by the Weibull distributed random numbers, which are calculated from the shape parameter k and the scale parameter λ for each class. Wind directions of each representative wind series are given by the statistical results of the 50-year wind data in each class (Figure 3a);
- (2) The generated Weibull random numbers (unit: m s^{-1}) are classified into 15 zones (from 0 m s^{-1} to 30 m s^{-1}) at intervals of 2 m s^{-1} ; next, these numbers are ‘marked’ by directions according to the statistics of the directional distributions within each speed zone based on the 50-year data. After this step all the wind elements (each with a speed and direction) are ready and then these elements need to be arranged to obtain a wind series. Usually, a real wind series is composed of a series of wind ‘sub-groups’ as shown in Figure 4. In this study, a wind sub-group is defined as an independent time series (event) in which the elements have similar directions. The range of a wind sub-group is restricted by either a transition of the wind direction ($\geq 45^\circ$) or a low wind speed ($\leq 3 \text{ m s}^{-1}$, as a wind speed of 3 m s^{-1} is not able to induce visible sediment transport). Eight direction groups are defined, named N-NE, NE-E, E-SE, SE-S, S-SW, SW-W, W-NW and NW-N; the wind elements are then reclassified into these 8 wind direction groups. The next step is to extract the sub-groups from the 8 large groups;

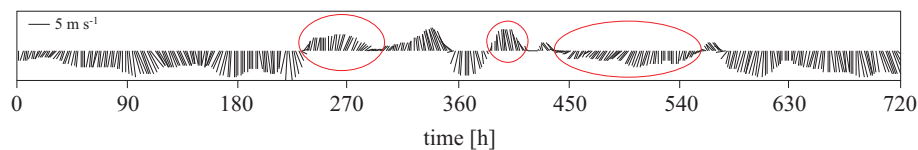


Figure 4. Example of a real wind series (January 2000). A wind sub-group is defined as an independent event (red circle). Elements within one sub-group have similar directions

- (3) The number of sub-groups has to be determined as it influences the wind fetch in the model calculation (i.e. a large sub-group which

contains a long series of wind elements with similar wind directions will induce larger wind fetch and stronger waves in the model calculation). As the research area is dominated by westerly winds, the division of the westerly wind sub-groups (SW–W and W–NW) is analysed. No division is carried out in the other groups (N–NE, NE–E, E–SE, SE–S, S–SW and NW–N). The resultant representative wind series for class 1 after step (2) and the division scheme of the westerly wind sub-groups are shown in Figure 5. Sensitivity experiments (which will be described in the following part) are carried out to obtain the optimum division of the westerly wind sub-groups capable of inducing approximate coastline change in the morphodynamic model compared to the measured data;

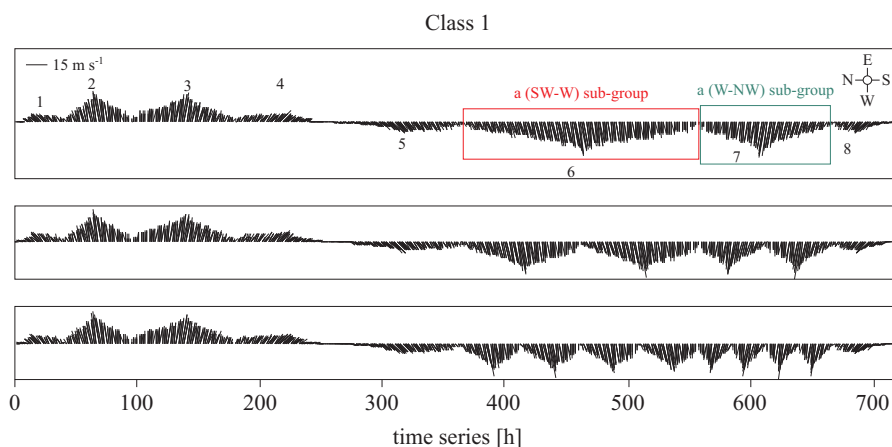


Figure 5. Top panel: Generated representative wind series for Class 1 after step 2. Middle panel: Division of the westerly wind sub-groups by a factor of two in representative wind series 1. Bottom panel: Division of the westerly wind sub-groups by a factor of four in representative wind series 1

- (4) When the optimum division of wind sub-groups is obtained through the sensitivity studies, the sub-groups of each representative wind series are arranged according to the short-term cyclical term on an hourly or daily scale, and the resultant representative series need to be further corrected by longer-term (yearly) trend and cyclical terms. Longer time scales of trend and cyclical terms that exceed the time span of the hindcast data (50 years) also need to be analysed according to the studies of long-term climate change. In our present study, the trend and cyclical term at scales longer than 50 years for the hindcast and projection of the 300 years' evolution of the Darss-Zingst peninsula are neglected and the normal wind conditions that exclude

storm information are assumed to be periodic every 50 years. This assumption is based on the analysis of the trends and cycles of the 50-year wind data, which is introduced as follows.

The yearly trend term of wind series is given by

$$\{V_{t+n}\} = \{V_t\} + m_{L,n}, \quad (7)$$

where $\{V_{t+n}\}$ represents the average value of wind series in the n^{th} time period (year), $\{V_t\}$ represents the average value of the first wind series (year), $m_{L,n}$ is the yearly trend term of the wind series. To determine the yearly trend terms, the Weibull parameters for each year from 1958 to 2007 are calculated. The linear best-fit functions of the parameters indicate very slight trend terms. For the scale parameter λ , the best-fit function is

$$y = 0.0004\chi - 0.03, \quad (8)$$

where y denotes the value of λ , and χ denotes the year (from 1958 to 2007). For the shape parameter k , the best-fit function is

$$y = 0.0004\chi + 1.447. \quad (9)$$

These trend terms are too small to be considered on a decadal-to-centennial scale, so the yearly-scale trend term of wind strength is assumed to be zero.

The cyclical term of wind series can be divided into a long-term (yearly) cyclical term ($S_{L,n}$) and a short-term (hourly to daily) cyclical term ($S_{L,h}$). The short-term cyclical term is obtained by calculating the autocorrelation coefficients of hourly wind speed and wind direction series with time lags from 1 hour to 8760 hours. Results show that the value of the autocorrelation coefficient decreases abruptly from 0.95 to 0.1 in the first 72 hours in both series, and is maintained in the range from -0.1 to 0.1 in lags from 72 to 8760 hours. The loss of correlation within a short time in both series indicates that there are no short-term cyclical terms in the wind series. The yearly cyclical term is shown in both class-averaged wind speed series and wind direction series, which indicates similarities of wind series within each class on a yearly scale. Based on the results of the cyclical terms, each representative wind series can be regarded as an independent series not correlated with the others.

With the information on trend and cyclical terms to hand, we can conclude a modelling strategy that the generated representative monthly wind series for each class, which serve as climate inputs for the model, is merely repeated in every cycle of model calculation (each cycle calculates one year's morphological change) without any trend correction. The same representative wind series are used in the hindcast of the last 300 years as well as the forward projection to the next 300 years. The use of the same

wind input conditions in the future projection is based on the IPCC (2007), which indicates that there are no consistent agreements on the future change of average or extreme wind speeds in Europe.

2.2.2. Storm analysis

Most information about extreme wind events is filtered in the generation of representative wind series, as extreme wind events make up only a small percentage of the whole time period. The statistics of hindcast wind data from 1958 to 2007 indicate that extreme wind events are frequent in the southern Baltic area and may play an important role in reshaping the coastline of the Darss-Zingst peninsula. Normally, the definition of a storm is related to water level variation and wind speeds. However, as only the wind data for this 50-year period are available, we here define a storm as a continuous time series with maximum wind speeds greater than 20 m s^{-1} , minimum wind speeds greater than 14 m s^{-1} and of duration longer than 24 hours. According to this criterion, 57 storms occurred in the Darss-Zingst area during 1958–2007, 8 of which were from the east and the rest from the west. Statistical results indicate that January and November can be described as storm months: 31 storms took place in this period. The distribution of storm directions indicates that WNW is the most probable direction for a storm in this area, with a percentage of 43%. The most probable direction for an easterly storm is NE, with a percentage of 65% in the 8 storms. The annual maximum wind speed profile indicates that storms occur almost every year and that there is no distinct trend in the variation of the storm strength in this 50-year period.

Extreme value theory is applied to analyse the storms. The Gumbel distribution is used to calculate the return period of storms. The probability density function of the Gumbel distribution is

$$f(\chi) = \frac{1}{\sigma} \exp \left[\frac{\mu - \chi}{\sigma} - \exp \left(\frac{\mu - \chi}{\sigma} \right) \right], \quad (10)$$

where σ is the scale parameter, μ is the location parameter, and χ is the maximum wind speed of the year.

The cumulative distribution function of the Gumbel distribution is given by

$$F(\chi) = \exp \left[- \exp \left(\frac{\mu - \chi}{\sigma} \right) \right]. \quad (11)$$

Following a double logarithmic transformation, eq. (11) can be written as

$$\ln[-\ln F(\chi)] = \frac{\mu - \chi}{\sigma}. \quad (12)$$

Knowing $F(\chi)$ and χ from the statistics of the annual maximum wind speed, the values of σ and μ can be obtained by least squares fitting using

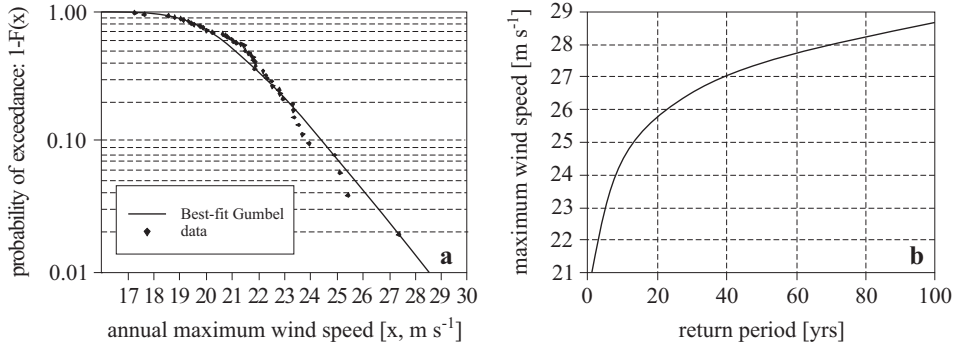


Figure 6. (a) Probability of the annual maximum wind speed being exceeded; (b) return periods of maximum wind speeds (b)

eq. (12). The best-fit Gumbel distribution of the annual maximum wind speed for the period of 1958–2007 is given by $\sigma = 1.498$ and $\mu = 20.49$. The resultant Gumbel fitting curve is shown in Figure 6a. The return period of the annual maximum wind speed is thus given by

$$R(\chi) = \frac{1}{1 - F(\chi)}. \tag{13}$$

The curve of $R(\chi)$ is shown in Figure 6b. Some maximum wind speeds with their return periods and probability of occurrence are listed in Table 3.

Table 3. Calculated return periods and probabilities of occurrence of annual maximum wind speeds on the Darss-Zingst peninsula based on 50-year data

Annual maximum wind speed [m s ⁻¹]	Return period [years]	Probability of occurrence [%]
28.6	100	1
27.4	50	1.8
26.2	25	1.8
25.8	20	3.5
24.5	10	7
23.1	5	17.5
21.5	2	47
18.3	1	96.5

It is not realistic for the morphodynamic model to include every wind storm with a different return period. According to the distribution of wind storm directions and the frequency of the storms that blew in the research area in the period of 1958–2007, one annual storm from the WNW and a once-every- n -years storm from the NE are included in the model. Here, n is a variable (which should range between 5 and 10 according to the

statistical result) that results from correction of the wind-induced wave spectrum aiming at inducing similar coastline change to the measured data. The maximum wind speed is 21.5 m s^{-1} in both storms and the duration is 48 hours (wind speed above 14 m s^{-1} , according to the definition of a storm), which is the typical duration of a storm in the southern Baltic Sea according to the statistical results of wind storms in 1958–2007. The wind speed is assumed to increase linearly from 14 m s^{-1} to 21.5 m s^{-1} and then decrease linearly to 14 m s^{-1} within this time span.

2.3. Calibration of the representative wind series

Four primary representative wind series are generated according to the methodology presented in section 3. However, these are not yet the final series serving for the model boundary input as the internal variation of these series such as the ordering of the wind sub-groups and the wind fetch (determined by the division of wind sub-groups) may significantly influence the simulation results. In order to obtain a wind series that induces a similar coastline change as the measured data (Figure 7), a series of model runs are carried out to test the sensitivity of the simulation results to the variation of the representative wind series.

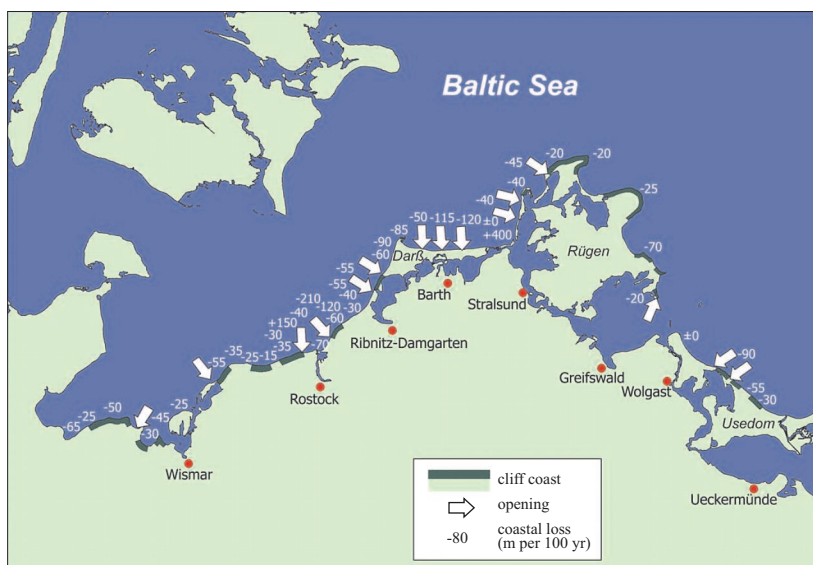


Figure 7. Measured coastline change of the Darß-Zingst peninsula in the 20th century (from the State Agency for Environment and Nature, Rostock (StAUN 1994)). A negative number denotes coastline retreat, a positive number denotes coastline accretion (m per 100 years)

The coastline change from 1900 to 2000 is modelled in a series of runs using different settings of wind input conditions. In the first set of runs, Run01, Run02 and Run03 have the same parameter setting except for the return periods of a north-easterly wind storm. Run01 does not include NE storm effects; Run02 considers a return period of 10 years of the NE storm, and Run03 considers a return period of 5 years of the NE storm. Comparisons of the model results are shown in Figure 8. The results demonstrate that north-easterly storms have significant effects on the Zingst coast (from Point 11 to 15) and exert a dominant influence on coastline change on Zingst. The coastline change induced by NE storms with a return period of 5 years (Run03) is nearly twice as much as that without NE storms (Run01) on Zingst. However, the other parts of the research area are not very sensitive to NE storms. These areas are reshaped mainly by the long-term effects of waves and longshore currents. Wind

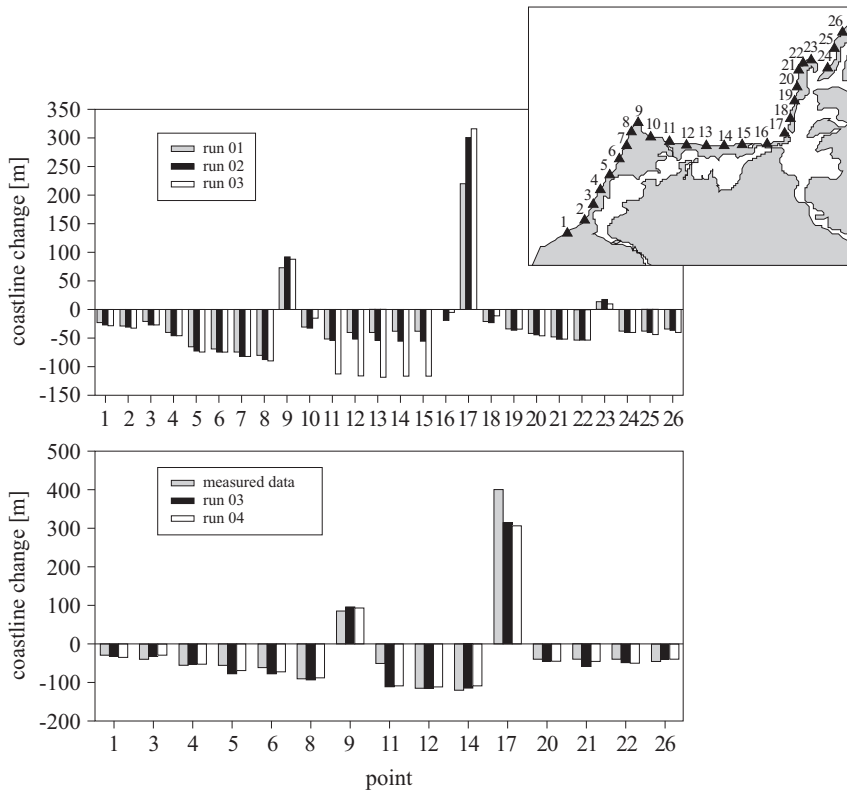


Figure 8. Top panel: Comparisons of model results with different parameterizations of storm frequency. Bottom panel: Comparisons of model results with different divisions of westerly wind sub-groups. The x-axis indicates the coastal points along the peninsula in both graphics

storms from the WNW increase these long-term effects and induce a ca 10% greater coastline change. The return period of 5 years of the NE storm in the model produces a similar coastline change to the measured data. The second set of runs is designed to test the sensitivity of coastline change to different divisions of the westerly wind sub-groups. These runs have the same parameter setting except for the division of the westerly wind sub-groups in the representative wind series. Run03 (the same run described in the first set) has no division of westerly wind sub-groups; Run04 has a division of the westerly wind sub-groups by a factor of two; Run05 has a division by a factor of four. Results indicate that the coastline along Darss faces more changes (either recession or accretion) under a longer westerly wind fetch (fewer divisions), but the trend decreases eastwards along Zingst to Hiddensee Island. Such a decreasing trend implies that the coastline at different sites responds differently to the wind fetch. The Darss coast is most sensitive to the westerly wind fetch because of its geographical position and relatively deep water environment; the Zingst coast is less sensitive to westerly winds owing to the sheltering effects of the headland; the nearshore area of Hiddensee is relatively shallow (mostly within 10 m), which causes a considerable dissipation of the energy of the waves before their arrival at the shoreline; hence less coastline change is induced along the island. A longer westerly wind fetch also induces more growth of the headland at the Darsser Ort and more sedimentation in the channel between Bock Island and Hiddensee. The division factor of two (Run04) of the westerly wind sub-groups in the representative wind series produces a better-fit coastline change to the measured data than the other two runs. In the third set of runs, Run03 (the same run as mentioned above), Run06 and Run07, the long-term effects caused by the different orderings of the wind sub-groups are calculated. Model results indicate that the long-term (100 years) coastline change is not very sensitive to the ordering of the wind sub-groups. Differences in the calculated bathymetric change at the same coastal profile are within 7% among the different model runs, and the differences in coastline change at the same point (the coastal points are indicated in Figure 8) are within 4%. This may be due to two reasons: (1) the repetitive cycles of calculation with these wind series smooth out the differences caused by different orderings of wind sub-groups and (2) the effects of the dominant westerly winds cannot be eliminated by different orderings of the wind sub-groups.

As a whole, Run04 (with a return period of 5 years for the NE storm and division of the westerly wind sub-groups by a factor of two) produces the best-fit coastline change to the measured data in the last century.

2.4. Validation of the representative wind series

A digital elevation model (DEM) of the research area for the year 1696 was reconstructed on the basis of high-resolution bathymetric and topographic data sets measured in modern times (Zhang et al. 2011). Based on the reconstructed DEM, a recent sediment map, an isostatic map, an eustatic scenario for the last three centuries (Meyer et al. 2008) and validated modules, the model was applied to hindcast the coastal evolution of the Darss-Zingst peninsula from 1696 to 2000 without taking into account anthropogenic influence (Zhang et al. 2011). The calibrated representative wind series serve as input conditions for the model. Successful validation of the representative wind series was shown by comparison between the modelled coastline change and the measured data along the peninsula with a RMSE = 61 m (which is about 1/5 of the averaged coastline change for the last 300 years). The simulated coastline in different time periods indicates a smooth evolution of the area in the last 300 years. Most of the coastline has been retreating except two parts: (1) the headland and its eastern side and (2) Bock Island. These two areas act like reservoirs where sediment converges, but the mechanisms driving their evolution are different. The growth of the headland is a combination of long-term wave dynamics (wave breaking, longshore currents) and short-term storm effects. The development of Bock is a residual effect of long-term wave dynamics (Zhang et al. 2010). The simulated results agree with other studies on the Darss-Zingst peninsula (Lampe 2002, Milbradt & Lehfled 2002, Froehle & Dimke 2008).

3. Results

Based on a successful validation, the model is used to project the morphological evolution of the Darss-Zingst peninsula during the next 300 years without consideration of any coastal protection measures. The effects of sea level rise and storm frequency on coastline change in the southern Baltic are quantified. Four different climate scenarios are designed, based on existing studies of climate change in the southern Baltic Sea or adjacent area (North Sea). All scenario runs use the same representative wind series described in section 3.1. The differences among these runs are the parameterization of the storm frequency and the rate of sea level change. The first scenario (Scenario 1) assumes an average sea level rise of 2 mm year⁻¹ (Meyer et al. 2008). The storm frequency in this run remains the same as the 50-year statistical results (i.e. an annual WNW storm and a once-every-5-years NE storm). Though there is little consistent evidence among different studies that shows changes in the projected frequency of

extreme wind events at either a global or a regional scale (IPCC 2007), in order to quantify the effects of storms on the coastline change, an increase of the storm frequency by 20% (both for storms from the WNW and the NE) compared to the 50-year results is assumed in the second climate scenario (Scenario 2). A sea level rise of 2 mm year⁻¹ is also parameterized in the second scenario. The third climate scenario (Scenario 3) assumes an average sea level rise of 3 mm year⁻¹ according to the projection results (1990–2100) of the sea levels of the Baltic Sea described in Meier et al. (2004). The storm frequency remains the same as the 50-year statistical results in the third scenario. In the fourth climate scenario (Scenario 4) both the rate of sea level rise and storm frequency are increased (i.e. a 3 mm year⁻¹ sea level rise and an increase in storm frequency by 20% compared to the 50-year data).

3.1. Morphological change

The coastline change in most parts of the peninsula is accelerated compared to the change in the last 300 years owing to the sea level rise in Scenario 1 (Figure 9). An increment of 10–15 m per 100 years in the coastline retreat on the Darss coast is anticipated compared to the rates of

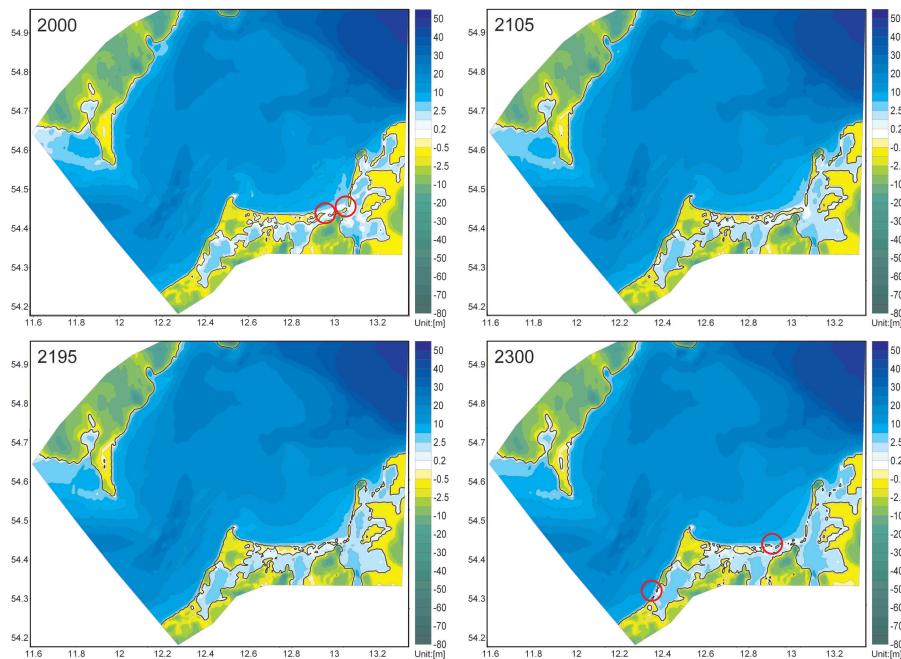


Figure 9. Projected coastal evolution of the Darss-Zingst peninsula in the next 300 years based on climate Scenario 1. The red circles indicate the active channels

the 20th century, whereas the coastline change on Zingst is more drastic with an increment of 20–30 m per 100 years. The headland is still growing in this period, but this tendency gradually slows down, partly due to the sea level rise, which counterbalances deposition to some extent, and partly due to the decrease in the sediment source, because some of the currents are directed into a new storm-generated channel in the middle part of Darss. There are two channels in the Bock area nowadays – one between Zingst and Bock and the other between Bock and Hiddensee. According to the model results, the channel between Bock and Zingst will silt up completely in the next 100 years, while the channel between Bock and Hiddensee will continue to exist for the first 100 years but will eventually close between 2100 and 2200. Two new channels, leading to more efficient water exchange between the inner lagoon and the outer sea, will be formed according to the projection results.

Compared to Scenario 1, an increase in storm frequency has conspicuous effects on coastline change, which are shown in the projection result of Scenario 2 (Figure 10). Erosion of the coastline is stronger than in Scenario 1 with about 35% more changes on average. The maximum increased retreats

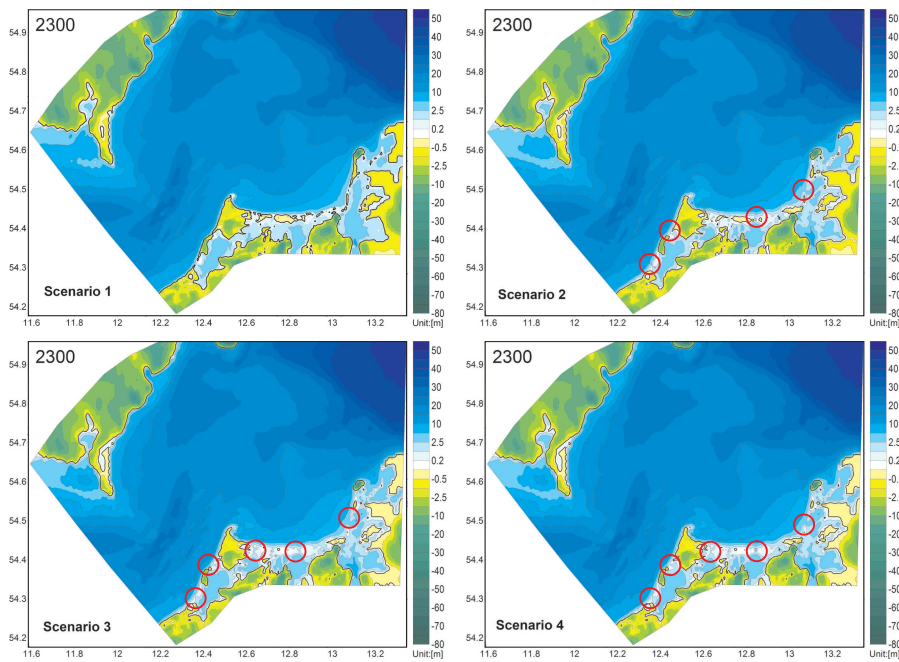


Figure 10. Comparison of the projected morphology of the Darss-Zingst peninsula in 2300 based on 4 different climate scenarios. The red circles indicate the active channels

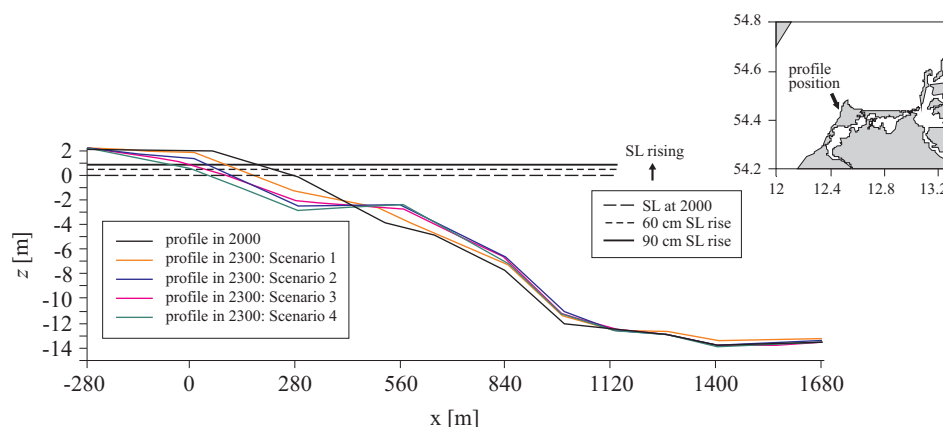


Figure 11. Comparison of the projected profiles of the Darss coast in 2300 based on 4 different climate scenarios

on the Darss and the Zingst coastlines are 97 m and 190 m respectively. In contrast to the stronger erosion on most parts of the coast, the growth of the headland and the Bock area is further developed in Scenario 2 compared to Scenario 1. An increased extension of 150 m of the headland compared to Scenario 1 is predicted in Scenario 2. Such growth is induced by the increased frequency of storms, especially from the west, which scour large amounts of sediment offshore from the shoreline area; these sediments are then gradually transported towards the headland by longshore currents. The increased sedimentation in the Bock area is a combination of storm effects from different directions (westerly and easterly). The westerly storms induce more deposition in the offshore area by erosion on the Hiddensee coastline, whereas the easterly ones are mainly responsible for erosion on the Zingst coastline, which provide additional sediment sources for the Bock area. Four new channels are created in Scenario 2, two of which are on the Darss coast, one on the Zingst coast and one on Hiddensee. These channels play a key role in changing the hydrodynamics and turning the inner lagoon system into an open environment that is more vulnerable to storm attack.

The effects of accelerated sea level rise (3 mm year^{-1}) on the coastline change are reflected in Scenario 3 (Figure 10). The coastline change caused by such an accelerated sea level rise is even more remarkable than that due merely to increased storm frequency (Scenario 2). Although the coastline of the whole area is facing more changes under the effects of accelerated sea level rise, different parts of the area respond differently. The coastline change on Darss in Scenario 3 is similar to Scenario 2, with an average increased retreat of 45 m compared to Scenario 2. The differences between these two scenarios become distinctive in the headland and the Zingst area.

The projected headland in Scenario 3 is much narrower than in Scenarios 1 and 2, even though it is still growing. An increased retreat of about 150 m in the western part and about 165 m in the eastern part of the headland (compared to Scenario 2) is projected in Scenario 3. The ‘thinning’ of the headland is caused mainly by the effects of accelerated sea level rise. As the sea level rises more rapidly than usual (Scenario 1), sediments (either from coastal erosion or supplied by longshore currents from other sources) become easier to trap in the deeper offshore area, where waves are difficult to reach (this can be identified from the profile changes shown in Figure 11). Trapping of sediment in the offshore area reduces the number of sources for the headland’s growth; on the other hand the rise of sea level further counterbalances the sedimentation around the headland. With a smaller sediment supply, the headland thus becomes ever narrower. The accelerated sea level rise is not only responsible for the ‘thinning’ of the headland, but also causes significant changes in the Zingst area: this is mostly submerged by water in Scenario 3, leaving only several discrete sand flats. Hiddensee suffers a similar fate and is split into two main islands. Five new channels are formed in Scenario 3, two of which are on Darss, two are on Zingst and one is in the Hiddensee area. The results of Scenario 3 also indicate that the Zingst coast is most sensitive to the accelerated sea level rise.

The projected coastline in Scenario 4 seems quite similar to Scenario 3, with minor differences (e.g. an average increased coastline retreat of 30 m on Darss compared to Scenario 3) in most parts. The largest difference of the coastline between these two scenarios lies in the headland. The headland projected by Scenario 4 becomes broader than in Scenario 3: this is due to the increased storm frequency, which provides additional sediment sources for the headland, even though a large part of the sediment is trapped in the offshore area. Another difference between Scenarios 3 and 4 is the offshore area. Scenario 4 induces more sedimentation in the offshore area as a result of the increased storm frequency. This is especially evident in the Zingst area, where the 5 m and 7.5 m isobaths extend about 190 m and 110 m northwards respectively.

3.2. Coastal profile change

A plot of the profiles perpendicular to the coastline can help to show more details of the cross-shore changes induced by different climate scenarios. In Figure 11, changes of the profile located on the Darss coast are compared. The horizontal resolution of the profiles is about 100 m in the coastline area (between -100 m and 500 m in the cross-shore direction shown in Figure 11) and gradually decreases to 300 m at the 13 m isobath. Resolution of the further offshore area is about 400 m. Projection results

indicate remarkable profile changes in the nearshore and offshore areas. All four scenarios anticipate erosion in the nearshore area (where the water depth is less than 3 m) and deposition in the adjacent offshore area. A longshore bar develops as a result of sedimentation in the offshore area. The position of the longshore bar is not always fixed: it moves upwards as the sea level rises, along with further development. The difference between the profiles in Scenarios 1 and 3 is remarkable, even though the sea level rise increases by just 30 cm in the latter. This is because the accelerated sea level rise enables waves to act further up the beach profile and cause stronger erosion. The increased storm frequency also causes significant changes on the profile. Scenario 2 produces a quite similar profile to Scenario 3. The similarity of profile change between these two scenarios indicates that an accelerated sea level rise of 3 mm year^{-1} and a 20% increase in storm frequency have almost the same effects on the coastline change of Darss. However, the combination of these two factors in Scenario 4 does not cause a linear effect in which the individual effects of these two factors on the profile can simply be summed. Comparison of Scenario 4 with the other two scenarios (Scenario 2 and 3) indicates that the profile evolves into an almost equilibrium state in these scenarios.

4. Discussion

4.1. Long-term modelling strategy

A long-term morphological simulation cannot take into account all the processes involved, especially those stochastic processes taking place on a short time scale (e.g. one heavy precipitation event) owing to a lack of data and practical run-time limits. In order to solve the problem of model input, concepts of ‘input reduction’ are implemented in our modelling work. ‘Input reduction’ refers to the filtering of the climate input conditions for a long-term model. Representative climate time series, which are generated by statistical analysis of the measured data and corrected by sensitivity studies, serve as input for the long-term model. A critical criterion for evaluating the reliability of the representative climate time series is whether the model computation with the representative input conditions produces similar results to the reference data. Thus, calibration and validation of the representative time series are very important before the final application of the model. Calibration of the representative wind series in this work is based on a series of sensitivity studies in which the effects of storm frequency, wind fetch and ordering of wind sub-groups on the coastline change are quantified. The representative wind series are validated by comparison between the model results and measured coastline change in

the last 300 years. Hindcast results indicate long-term wave dynamics (wave breaking, longshore currents) and short-term storms as two dominant factors influencing the coastline change of the Darss-Zingst peninsula in the last three centuries. Compared to these two factors, long-term sea level change played a minor role in driving coastal evolution in this time period because of its relatively low rate, which is about 1 mm year^{-1} according to Hupfer et al. (eds.) (2003) and Ekman (2009).

Morphodynamic evolution of the Darss-Zingst coastline is significantly influenced by regional climate factors such as sea level change and winds. To represent the climate factors as input for the long-term model, hourly wind series for a 50-year period (1958–2008) are analysed to generate the representative time series; waves and currents are calculated in the model using the wind field as input; the long-term (centennial) sea level change is parameterized on the basis of existing climate studies (Voss et al. 1997, Meier et al. 2004, IPCC 2007). Although satisfactory hindcast results are produced, the influences of other factors such as coastal engineering work on coastline change need to be carefully evaluated when the model is used for future projections. Coastal engineering work has provided additional protection for the Darss-Zingst coastline since the last century (Froehle & Kohlhasse 2004) and will continue to do so for the foreseeable future. Such anthropogenic influence is excluded in our model, as projection results without anthropogenic influence should help to make coastal management more efficient by indicating how nature acts on coastline change, thus providing useful information for coastal engineering work.

4.2. Storm effects on long-term coastline change

Our model results suggest that both accelerated sea level rise and increased storm frequency have significant effects on the coastline erosion of the Darss-Zingst peninsula on a centennial scale. The effect of sea level rise on long-term coastline change is commonly recognized in current studies. However, the effects of storms on the long-term coastline change indicated in our model results seem to be inconsistent with some other studies (Douglas & Crowell 2000, Zhang et al. 2002) in which storm erosion of the beach was found to be episodic but not secular, as the beach profile recovers after each storm. Actually, the importance of storm effects on the coastline change found in this study does not conflict with the studies mentioned above, as there are many differences between the research areas. In a study on the Texas coast Morton et al. (1994) discovered four dominant processes in beach recovery: (1) rapid forebeach accretion under mild weather conditions, (2) backbeach aggradation, (3) dune formation and (4) dune expansion and vegetation recolonization. They also found that

post-storm beach responses at individual sites are highly variable and that not all beach segments can recover after storm erosion. Several conditions have to be satisfied for the complete recovery of a beach profile: (1) a long enough time interval between two storms (usually several years or even more, depending on the local environment), (2) a stable hydrodynamic environment, and (3) a sufficient sediment supply. The preconditions for beach recovery are not fulfilled in our research area as the southern Baltic Sea is characterized by strong wind conditions with storms almost every year. Insufficient sediment sources (partly blocked by the headland and partly trapped in the offshore area) make complete beach recovery in this area even more difficult. Therefore, storm-induced erosion on the coastline of the Darss-Zingst peninsula is a long-term factor and cannot be neglected.

4.3. Shortcomings and future work

The shortcomings of a numerical model (especially a long-term model) can be as remarkable as its advantages when it is used to simulate real nature. Biased results are generally caused by (1) too coarse a resolution of the model domain in which small-scale details are excluded or smoothed, (2) biased parameterization and boundary inputs, which can lead to significant differences between the model results even if they are based on the same equations; such effects can be greatly amplified during a long-term run, (3) scant knowledge of interactions between different scale processes, and (4) the deterministic results of process-based models, in which the stochastic dimension inherent to the natural systems we are working with is ignored (de Vriend 2001). Climate change is assumed to be linear, and short-term fluctuations are excluded from our current modelling work. The authors admit that there is large uncertainty of climate change in the future and it is not possible to specify accurate climate input conditions for future predictions. Thus, our results are projection results based on certain particular climate scenarios rather than accurate future predictions. The aim of this study is to identify the key coastal areas most vulnerable to climate change impacts, such as accelerated sea level rise and increased storm frequency, and reveal the nonlinear effects on the coastal morphological evolution caused by these climate factors. Although uncertainty of climate change exists, the hypothesis of linear climate change seems to be acceptable for the simulation of the Darss-Zingst peninsula from 1696 to 2300. This is probably due to two main reasons: (1) the research area has a relatively stable coastline boundary, which does not allow for much change caused by stochastic climate fluctuations; (2) studies of the North Atlantic Oscillation (NAO), which turns out to be an important factor influencing the climate of the Baltic Sea in winter (Klavins et al. 2009),

indicate that although variability has existed on an annual scale during the last two centuries (HELCOM 2006), the 30-year averaged NAO index series of the last three centuries fluctuates slightly from the value of zero (Trouet et al. 2009). This supports the feasibility of periodic climate inputs generated on the basis of the 50-year wind data analysis for the historical hindcast or future projection on a centennial scale in the model. However, this hypothesis may be violated when the model is applied to a longer time span (millennial scale), as the model boundary is more variable and the non-linear effects caused by the linear parameterization of climate conditions can accumulate and may ultimately dominate the results. The estimation and quantification of these uncertainties for the simulation of millennial-scale coastal evolution (either hindcast or prediction) remain a challenge for our model work.

Our model only includes hydrodynamic driving forces (waves, currents and storms), long-term climate factors (sea level change) and neotectonic movements controlling coastal evolution, but ignores some other natural processes that may also have a significant influence on long-term coastline change; for example, aeolian accumulation and erosion of sand dunes, biological factors influencing sediment transport, protection of the cliff and land by vegetation, potential erosion of the cliff caused by underground water and ice cover. One topic of our future research work will focus on improving the model by integrating these processes, especially aeolian sand transport, which is closely related to beach recovery.

5. Summary

A modelling methodology for simulating the decadal-to-centennial morphological evolution of the wave-dominated southern Baltic coast has been developed. A method for generating representative climate conditions serving for the model boundary input is presented in this paper. The method is based on the statistical analysis of 50-year high-resolution (hourly averaged) wind data. Four seasonal wind classes, each with a predominant distribution of wind direction and speed, are derived. The Weibull distribution function is used to analyse the wind strength of each class. The Weibull distributed random number generator is applied to generate the representative wind series based on the Weibull parameters of each class. Long-term trend terms of the wind series are analysed by linear best-fit functions of the yearly Weibull parameters. Auto-correlation coefficients are calculated to obtain the cyclical terms of the wind series. Extreme value theory serves as a tool to calculate the return periods of storms. The generated wind series (including the representative storms) are further calibrated by sensitivity studies of the model. After a successful model

validation, coastline change of the Darss-Zingst peninsula in the next 300 years is projected on the basis of four different climate scenarios, through which impacts of long-term sea level change and frequency of storms on the coastline change are quantified. The projected coastline change in most parts of the peninsula is faster than the change in the last 300 years in all climate scenarios as a result of sea level rise. An 20% increase in storm frequency (Scenario 2) induces a ca 35% greater coastline retreat (compared to Scenario 1) when the rate of sea level rise is 2 mm year⁻¹; however, such storm-induced effects become less remarkable under an accelerated sea level rise of 3 mm year⁻¹. The increase in storm frequency by 20% in Scenario 4 induces only a ca 11% greater coastline change than Scenario 3. Comparison of Scenario 4 with two other scenarios (Scenario 2 and 3) indicates that the coastal profile on Darss will evolve into an almost equilibrium state in these scenarios.

Acknowledgements

The hindcast wind data (1958–2007) of the Baltic Sea were kindly provided by Dr. R. Weisse. The simulations were carried out at the supercomputing facilities of the MPI-IPP (Max-Planck-Institute for Plasma Physics) in Greifswald and Garching, Germany. The research work is supported by the SINCOS project. One of the authors (Zhang, W. Y.) was supported by a scholarship offered by the China Scholarship Council (CSC).

References

- Cayocca F., 2001, *Long-term morphological modeling of a tidal inlet: the Arcachon Basin, France*, *Coast. Eng.*, 42 (2), 115–142.
- de Vriend H. J., 2001, *Long-term morphological prediction*, [in:] *River, coastal and estuarine morpho-dynamics*, G. Seminara & P. Blondeaux (eds.), Springer, Berlin, 223 pp.
- de Vriend H. J., Copabianco M., Chesher T., De Swart H. E., Latteux B., Stive M. J. F., 1993a, *Approaches to long-term modelling of coastal morphology: a review*, *Coast. Eng.*, 21 (1–3), 225–269.
- de Vriend H. J., Zyserman J., Nicholson J., Roelvink J. A., Pechon P., Southgate H. N., 1993b, *Medium term 2DH coastal area modelling*, *Coastal Eng.*, 21 (1–3), 193–224.
- Dastgheib A., Roelvink J. A., Wang Z. B., 2008, *Long term process-based morphological modelling of the Marsdiep tidal basin*, *Mar. Geol.*, 256 (1–4), 90–100, doi: 10.1016/j.margeo.2008.1003.

- Dissanayake D.M.P.K., Roelvink J.A., 2007, *Process-based approach on tidal inlet evolution – Part 1*, Proc. 5th Symp. ‘River, coastal and estuarine morphodynamics’, 225–269.
- Douglas B.C., Crowell M., 2000, *Long-term shoreline position prediction and error propagation*, J. Coast. Res., 16 (1), 145–152.
- Ekman M., 2009, *The changing level of the Baltic Sea during 300 years: A clue to understanding the Earth*, Summer Inst. Historical Geophys., Åland Islands, 155 pp.
- Fagherazzi S., Overeem I., 2007, *Models of deltaic and inner continental shelf landform evolution*, Annu. Rev. Earth Pl. Sci., 35 (1), 685–715, doi: 10.1146/annurev.earth.35.031306.140128.
- Froehle P., Dimke S., 2008, *Analysis of potential long shore sediment transport at the coast of Mecklenburg-Vorpommern*, [in:] Proc. Chinese-German Joint Symposium of Hydraulic and Ocean Engineering, U. Zanke et al. (eds.), Inst. Hydraulic and Water Resources Engineering (Hrsg.).
- Froehle P., Kohlhas S., 2004, *The role of coastal engineering in integrated coastal zone management*, Coast. Rep. 2, 167–173.
- Harff J., Lemke W., Lampe R., Lüth F., Lübke H., Meyer M., Tauber F., Schmölcke U., 2007, *The Baltic Sea coast-A model of interrelations among geosphere, climate, and anthroposphere*, [in:] *Coastline changes: Interrelation of climate and geological processes*, J. Harff, W. W. Hay & D. M. Tetzlaff (eds.), Geol. Soc. Am. (GSA) Spec. Papers 426, 133–142
- HELCOM, 2006, *Climate change in the Baltic Sea area*, HELCOM Stakeholder Conf. ‘Baltic Sea action plan’, HELCOM thematic assessment in 2006, Helsinki Commiss., Helsinki.
- Hupfer P., Harff J., Sterr H., Stigge H.-J. (eds.), 2003, *Die Wasserstände an der Ostseeküste. Entwicklung – Sturmfluten – Klimawandel*, Archiv für Forschung und Technik an der Nord- und Ostsee, Die Küste H. 66, 331 pp., Boyens & Co. KG, Heide i. Holstein.
- IPCC, 2007, *Climate change 2007: The physical science basis*, Contribution of Working Group I to the Fourth Assessment Report of the Intergovernmental Panel on Climate Change, Cambridge Univ. Press, Cambridge.
- Jiménez J. A., Arcilla A. S., 2004, *A long-term (decadal scale) evolution model for microtidal barrier systems*, Coast. Eng., 51 (8–9), 749–764.
- Jones O.P., Petersen O.S., Hansen H.K., 2007, *Modelling of complex coastal environments: Some considerations for best practise*, Coast. Eng., 54 (10), 717–733.
- Klavins M., Briede A., Rodinov V., 2009, *Long term changes in ice and discharge regime of rivers in the Baltic region in relation to climatic variability*, Clim. Change, 95 (3–4), 485–498.
- Kliewe H., 1995, *Zeit- und Klimamarken in Sedimenten der südlichen Ostsee und ihrer Vorpommerschen Boddenküste*, J. Coast. Res., Special Issue. 17, 181–186.
- Kolp O., 1978, *Das Wachstum der Landspitze Darsser Ort*, Petermanns Geographische Mitteilungen 122, 103–111.

- Lampe R., 2002, *Holocene evolution and coastal dynamics of the Fischland Darss Zingst peninsula*, Greifswald Geographische Arbeiten, 27, D1, 155–163.
- Lampe R., 2005, *Late-glacial and Holocene water-level variations along the NE German Baltic Sea coast: review and new results*, Quatern. Int. Vol. 133–134, 121–136.
- Latteaux B., 1995, *Techniques for long-term morphological simulation under tidal action*, Mar. Geol., 126 (1–4), 129–141.
- Meier H. E. M., Broman B., Kjellström, E., 2004, *Simulated sea level in past and future climates of the Baltic Sea*, Climate Res., 27 (1), 59–75.
- Meyer M., Harff J., Gogina M., Barthel A., 2008, *Coastline changes of the Darss-Zingst peninsula – a modeling approach*, J. Marine Syst., 74 (Suppl. 1), S147–S154.
- Milbradt P., Lehfeldt R., 2002, *Littoral processes at micro-tidal coasts of the southern Baltic Sea*, Adv. Hydro-Sci. Eng.
- Morton R. A., Paine J. G., Gibeaut J. G., 1994, *Stages and durations of post-storm beach recovery, southeasterly Texas coast, U.S.A.*, J. Coast. Res., 10 (4), 884–908.
- Otto T., 1913, *Der Darss und Zingst: Ein Beitrag zur Entwicklungsgeschichte der vorpommerschen Küste. 13.*, Jahresber. Geogr. Ges. Greifswald, 1911–1912, 237–485.
- Roelvink J. A., 2006, *Coastal morphodynamic evolution techniques*, Coast. Eng., 53 (2–3), 277–287.
- StAUN – State Agency for Environment and Nature (StAUN) Rostock, 1994, Generalplan Küsten- und Hochwasserschutz Mecklenburg-Vorpommern, Landesentwicklung und Umwelt Mecklenburg-Vorpommern, Ministerium für Bau, 108 pp.
- Schiewer U., 2008, *Chapter 2: The Baltic coastal zones*, [in:] *Ecology of Baltic coastal waters*, Springer, doi: 10.1007/978-3-540-73524-3.
- Schumacher W., 2002, *Coastal evolution of the Darss Peninsula*, Greifswalder Geographische Arbeiten, 27, D2, 165–168.
- Schumacher W., Bayerl K.-A., 1999, *The shoreline displacement curve of Ruegen Island (Southern Baltic Sea)*, Quatern. Int., 56 (1), 107–113, doi: 10.1016/S1040-6182(98)00027-5.
- Schwarzer K., Diesing M., 2003, *Coastline evolution at different time scales – examples from the Pomeranian Bight, southern Baltic Sea*, Mar. Geol., 194 (1–2), 79–101.
- Trouet V., Esper J., Graham N. E., Baker A., Scourse J. D., Frank D. C., 2009, *Persistent positive North Atlantic Oscillation mode dominated the Medieval Climate Anomaly*, Science, 324 (50)2009, 78.
- Voss R., Mikolajewicz U., Cubasch U., 1997, *Langfristige Klimaänderungen durch den Anstieg der CO₂-Konzentration in einem gekoppelten Atmosphäre-Ozean-Modell*, Ann. Meteorol., 34, 3–4.

- Weisse R., Guenther H., 2007, *Wave climate and long-term changes for the Southern North Sea obtained from a high-resolution hindcast 1958–2002*, Ocean Dynam., 57 (3), 161–172.
- Weisse R., v. Storch H., Callies U., Chrastansky A., Feser F., Grabemann I., Guenther H., Pluess A., Stoye T., Tellkamp J., Winterfeldt J., Woth K., 2009, *Regional meteo-marine reanalyses and climate change projections: Results for Northern Europe and potentials for coastal and offshore applications*, Bull. Am. Meteorol. Soc., 90, 849–860.
- Wu C.Y., Bao Y., Ren J., Shi H.Y., 2006, *A numerical simulation and morphodynamic analysis on the evolution of the Zhujiang River Delta in China: 6000~2500 a BP*, Acta Oceanol. Sinica, 28 (4), 64–80.
- Zhang K.Q., Douglas B., Leatherman S., 2002, *Do storms cause long-term beach erosion along the U.S. East barrier coast?*, J. Geology, 110 (4), 493–502.
- Zhang W. Y., Harff J., Schneider R., Wu C. Y., 2010, *Development of a modelling methodology for simulation of long-term morphological evolution of the southern Baltic coast*, Ocean Dynam., 60 (5), 1085–1114, doi: 10.1007/s10236-010-0311-5.
- Zhang W.Y., Harff J., Schneider R., Wu C.Y, 2011, *A multi-scale centennial morphodynamic model for the southern Baltic coast*, J. Coast. Res., doi: 10.2112/jcoastres-d-10-00055.1.